Available online at www.sciencedirect.com
SCIENCE DIRECT®
ELSEVIER
Earth and Planetary Science Letters 214 (2003) 75–91
EPSL
www.elsevier.com/locate/epsl

Rapid eruption of Siberian flood-volcanic rocks and evidence for coincidence with the Permian–Triassic boundary and mass extinction at 251 Ma

Sandra L. Kamo [a,*], Gerald K. Czamanske [b], Yuri Amelin [a,1], Valeri A. Fedorenko [c], D.W. Davis [a], V.R. Trofimov [c]

[a] *Jack Satterly Geochronology Laboratory, Royal Ontario Museum, 100 Queen's Park, Toronto, ON, Canada M5S 2C6*
[b] *750 West Greenwich Place, Palo Alto, CA 94303, USA*
[c] *Central Research Institute of Geological Prospecting for Base and Precious Metals (TsNIGRI), Varshavskoye Shosse 129B, 113545 Moscow, Russia*

Received 27 August 2002; received in revised form 12 May 2003; accepted 9 June 2003

Abstract

The Siberian flood-volcanic event is the most voluminous and explosive, continental, volcanic event known in the Phanerozoic record. U–Pb perovskite and zircon ages were obtained for lavas of the lowermost unit (251.7 ± 0.4 Ma) and near-uppermost unit (251.1 ± 0.3 Ma), respectively, of the volcanic sequence in the Maymecha–Kotuy area, Russia. Along with stratigraphic correlations and paleomagnetic evidence, these ages suggest that rapid extrusion of the entire ~6500 m thick composite sequence occurred in less than 1 million years. The time of extrusion coincides precisely with an age of 251.4 ± 0.3 Ma previously obtained for the Permian–Triassic mass-extinction event, the most devastating biotic crisis known. Emplacement of the Noril'sk–Talnakh ore-bearing intrusions, notable for their prodigious Cu–Ni–PGE deposits, was synchronous with these two major geologic events at 251.2 ± 0.3 Ma. The Guli volcanic-intrusive complex in the Maymecha–Kotuy area appears to represent the final mafic magmatism of the entire Siberian flood-volcanic event. Baddeleyite from a carbonatite that intrudes the complex gives an age of 250.2 ± 0.3 Ma, and shows possible ^{231}Pa excess. The Bolgokhtokh granodiorite stock has a zircon age of 229.0 ± 0.4 Ma, and represents the youngest known magmatism in the region.

Keywords: U–Pb ages; Siberian flood volcanism; Permo–Triassic boundary; Perovskite; Zircon

1. Introduction

The timing and consequences of the massive, explosive eruption of the Siberian flood-volcanic rocks have been the subject of much discussion due to their suspected causal relation with the end-Permian mass-extinction event [1–10]. It is the largest subaerial volcanic event known, although the original volume of more ancient events

* Corresponding author. Tel.: +1-416-586-5783; Fax: +1-416-586-5814.
E-mail addresses: sandrak@rom.on.ca (S.L. Kamo), czamrandg@earthlink.net (G.K. Czamanske), yamelin@nrcan.gc.ca (Y. Amelin), vfedorenko@rambler.ru (V.A. Fedorenko).

[1] Present address: Geological Survey of Canada, 601 Booth Street, Ottawa, ON, Canada K1A 0E8.

0012-821X/03/$ – see front matter © 2003 Elsevier B.V. All rights reserved.
doi:10.1016/S0012-821X(03)00347-9

is difficult to determine because of erosion. Considering the coeval, mafic volcanic and intrusive formations known on the Siberian Platform, the Taymyr Peninsula, and the Western Siberian Lowlands, Masaitis [11] estimated their volume as $\sim 4\times10^6$ km^3, originally extending over $\sim 7\times10^6$ km^2. Reichow et al. [9] confirmed that the extensive, buried basalts in the Western Siberian Lowlands are coeval with the basalts on the platform.

The most intensely studied part of the Siberian flood-volcanic province is in the Noril'sk area, renowned for its prodigious Cu–Ni–PGE sulfide deposits. The Noril'sk I intrusion, which cuts the lower third of the volcanic sequence near Noril'sk, was dated at 251.2 ± 0.3 Ma [6] (2σ errors used here and throughout) by U–Pb on zircon and baddeleyite. The Maymecha–Kotuy area, located 500 km east-northeast of Noril'sk (Fig. 1), has received considerably less attention. Geochemical and petrographic correlation with the sequence at Noril'sk [12], in combination with previous paleomagnetic work [13], suggests that as much as 3000 m of volcanic stratigraphy in the Maymecha–Kotuy area is younger than the ~3500 m lava sequence at Noril'sk. This provides an estimate of ~6500 m for a maximal, composite section of the Siberian flood-volcanic sequence (Fig. 2A,B; [12,14]).

Prior to evaluating the potential environmental impact that Siberian flood volcanism may have had on the biota of the Pangean supercontinent, it must first be established beyond doubt that the two events occurred at the same time, or that volcanism slightly pre-dated the extinction event. This requires unequivocal, accurate, and precise ages for the two events from well-defined stratigraphic units.

The objectives of this study were: (1) to determine absolute ages for, and the duration of, the voluminous Siberian flood-volcanic event from a locality where a near-complete record of this volcanism is preserved; and (2) to establish the timing of this volcanism with respect to the age of the Noril'sk-type ore-bearing intrusions and the Permian–Triassic mass-extinction event. The U–Pb isotope-dilution, thermal ionization mass spectrometry (IDTIMS) dating method was used on

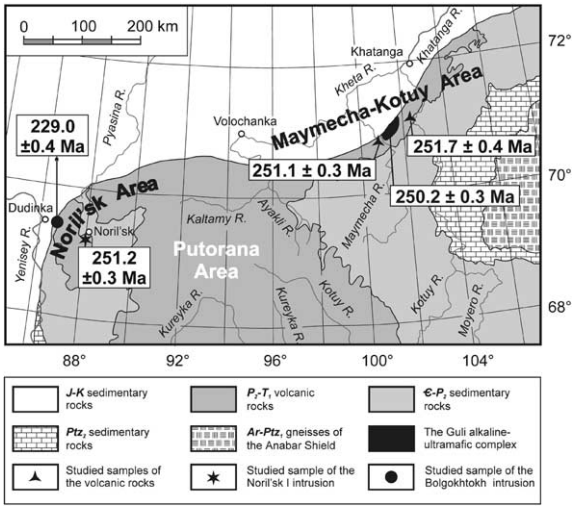

Fig. 1. Geologic map of the northwestern part of the Siberian Platform showing the distribution of Paleozoic sedimentary rocks and Siberian flood-volcanic rocks in the Maymecha–Kotuy and Noril'sk areas. To the east of these areas are Proterozoic sedimentary rocks and Archean gneisses of the Anabar Shield. Sample locations for the studied samples are indicated.

zircon, perovskite, and baddeleyite. Previous reports of U–Pb perovskite dating are limited to a few IDTIMS studies for kimberlites (e.g. [15–17]), and lamprophyre dykes [18], as well as two SHRIMP studies of kimberlite [19,20]. The ^{207}Pb/^{206}Pb ages and ^{207}Pb/^{235}U ages are relatively imprecise in this age range. However, high-precision ^{206}Pb/^{238}U ages (i.e. with errors of 0.1–0.5%) can be routinely obtained by using IDTIMS methods, even on single crystals of zircon.

2. Geologic background and sampling

The Maymecha–Kotuy area comprises ~70 000 km^2 of the northeastern part of the Siberian flood-volcanic province (Fig. 1). The geology of this area is characterized by the predominance of high-Ti, alkaline–ultramafic lavas and intrusive rocks over tholeiitic lavas, a marked contrast with the Noril'sk area [12]. Unique to the area are rocks that comprise the trachyandesite–trachyrhyodacite series, mela-nephelinites, meymechites, and alkaline–ultramafic intrusive complexes. This is the type locality of meymechitic

lava (e.g. [21]), which is not documented elsewhere. The volcanic sequence preserved in the Maymecha–Kotuy area rests with minor disconformity upon Permian sandstones, argillites, and coals of the Tungusskaya Series [22], as does the sequence in the Noril'sk area (e.g. [12]). The Maymecha–Kotuy volcanic sequence is divided into six suites that have been correlated with the suites of the Noril'sk area [12], as shown in Fig. 2A. Descriptions of the suites are given in Fig. 2B. The relation between the two sequences is based upon correlation of (1) the high-Ti units atop the Pravoboyarsky and Morongovsky suites; (2) the Onkuchaksky Suite with the Mokulaevsky through Samoedsky suites; and (3) geochemical and paleomagnetic correlation of the Tyvankitsky basalts with the Daldykansky intrusions at Noril'sk. In addition, the Noril'sk-type, ore-bearing and Lower Talnakh-type intrusions are considered to be coeval with the thick tuff unit that lies between the two Morongovsky Subsuites.

Although the maximal thickness of the Maymecha–Kotuy sequence is >4000 m, the thickest sections of the Delkansky and Maymechinsky suites predominantly fill local volcano-tectonic depressions and have areal extents of only several tens of kilometers. The thickness of the broadly spread volcanic cover is ~1800 m. Except for much of the Maymechinsky Suite, the lavas are well-developed flows with amygdaloidal zones in their upper parts, as is typical of lava flows in the Noril'sk area. The sequence is cut by numerous dikes and sills that occur in six widely separated localities, and have been subdivided into seven compositional types [12]. The latest volcanic activity occurs in multi-phase, intrusive-volcanic complexes. The largest of these is the Guli complex [12], which is cut by two carbonatite plugs.

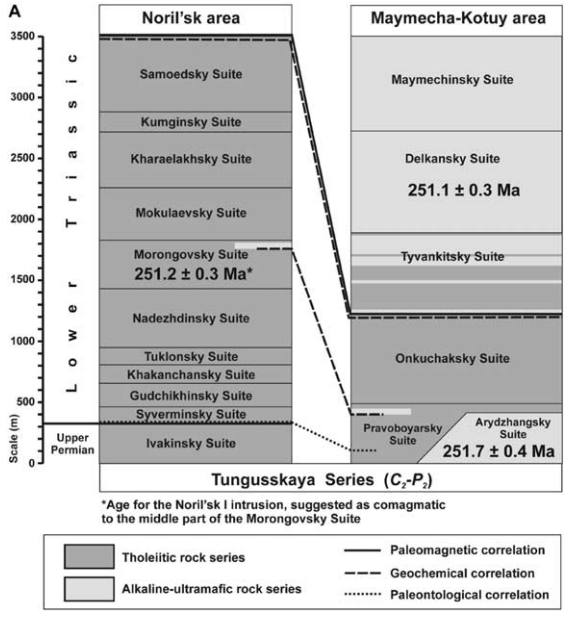

B

	NORIL'SK AREA	MAYMECHA-KOTUY AREA	
Late Triassic	***Bolgokhtokh***-type intrusions. Granodiorite. NMP	No magmatic activity	
Middle Triassic	No magmatic activity		
Early Triassic		Complex alkalic-ultramafic intrusions with carbonatite facies. RMP	
		Type-7 dikes (the ***Ust'delkansky type***). Trachydolerite. RMP. These cut the Maymechinsky meymechites, but their age relation to the complex intrusions is not known	
		Maymechinsky volcanic Suite. Meymechites; picrites and limburgites in the lower part. 1400 m. RMP	
	Avamsky-type dikes. Dolerite. RMP	***Type-4*** dikes (the ***Delakagsky*** type). Dolerite. RMP. These cut the lower part of the Delkansky Suite; their age with respect to the younger volcanic suites is not known	
		Delkansky volcanic Suite. Mela-nephelinitic lavas with rare trachyitic to trachyrhyodacitic tuffs and lavas in the lower part. The middle part is poor exposed. Trachybasaltic and trachyandesitic lavas are present in the upper part. 850 m. RMP	
	Daldykansky-type (doleritic) and ***Ruinny***-type (doleritic to picritic doleritic) intrusions. RMP	***Tyvankitsky*** volcanic Suite. Alternation of basalts with trachybasalts, trachyandesites, and trachytes. 700 m. RMP	
	Samoedsky and ***Kumginsky*** volcanic Suites. Basalts, 800 m. NMP	***Onkuchaksky*** volcanic Suite. Basalts. 750 m. NMP	
	Kharaelakhsky volcanic Suite. Basalts, thin ***Ikonsky*** leucocratic basalts in the upper part. 475-600 m. NMP. Remains of the mammal-like synapsid *Lystrosaurus? Cope*, belonging to the lower third of the Lower Triassic		
	Mokulaevsky volcanic Suite. Basalts. 400-670 m. NMP		
	Morongovsky volcanic Suite. Basalts with ***Yuryakhsky*** leucocratic basalts and ***Kaltaminsky*** ankaramites in the upper part. 250-700 m. NMP. It is suggested that the ore-bearing ***Noril'sk***-type intrusions are coeval with a thick tuff in the middle part of the Morongovsky Suite.	**At Maymecha River**	**At Kotuy River**
		Pravoboyarsky volcanic Suite. Basaltic tuffs, 15 m.	
	Khakanchansky, ***Tuklonsky***, and ***Nadezhdinsky*** volcanic Suites. Basaltic lavas and tuffs with picritic basalts in the Tuklonsky Suite. 150-600 m. NMP	***Pravoboyarsky*** volcanic Suite. Basaltic tuffs, tuffites. Rare flows (sills) of ankaramite-like rocks, similar to the Kaltaminsky ankaramites in the upper part. 320 m.	***Arydzhangsky*** volcanic Suite. Melilite-bearing mela- nephelinitic lavas. 330 m. NMP
	Gudchikhinsky volcanic Suite. Basalts and picritic basalts. 0-250 m. NMP		
	Syverminsky volcanic Suite. Basalts. 0-195 m. NMP		
Late Permian	***Middle*** and ***Upper Ivakinsky*** volcanic Subsuites. Leucocratic basalts. 0-150 m. RMP		
	Lower Ivakinsky volcanic Subsuite. Leucocratic trachybasalts. 0-240. The Ergalakhsky-1 type intrusions (leucocratic trachydolerites, NMP) are comagmatic with this Subsuite		
	Tungusskaya Series (C_2-P_2 coal-bearing sedimentary rocks)		

Fig. 2. (A) Stratigraphic correlation between the volcanic suites of the Maymecha–Kotuy and Noril'sk areas. (B) Description of the volcanic sequences in the Maymecha–Kotuy and Noril'sk areas and their correlation. Lavas designated as having normal (NMP) or reverse (RMP) magnetic polarity. These figures are based on the reports of Fedorenko and Czamanske [12] and Fedorenko et al. [14].

The onset of Siberian flood volcanism would be established by obtaining an age for the Ivakinsky Suite (or the co-magmatic Ergalakhsky-1 type intrusions) of the Noril'sk area, or the Arydzhangsky Suite of the Maymecha–Kotuy area (Fig. 2). Cessation of major volcanic activity could be established in the Maymecha–Kotuy area with ages for the type-7 trachydolerite dikes which cut the entire Maymechinsky Suite (thus were emplaced after eruption of the entire volcanic sequence in the Maymecha River basin) or for carbonatite from the Guli intrusive-volcanic complex, which is also considered to post-date lava accumulation. Less constraining would be an age for the trachydacites and trachyrhyodacites of the middle Delkansky Suite, which had been found to contain zircon in thin section. Exclusive focus was placed on the Maymecha–Kotuy area when samples of Ergalaksky-1 trachydolerite (from core NM-2, depth 735–750 m, 30 km north of Lake Keta), Upper Ivakinsky basaltic andesite (from the uppermost flow at Sondra Creek near the Noril'sk II intrusion) and type-7 trachydolerite (from the north end of the Ust'–Delkan dike-in-dike complex at the Maymecha River (figure 4 in [12]), yielded no suitable, datable material.

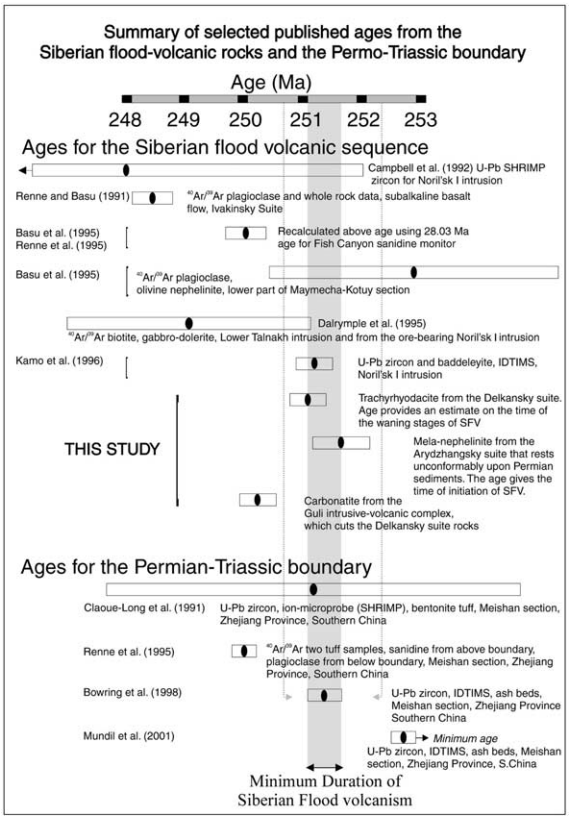

Fig. 3. Summary chart of ages for Siberian flood-volcanic rocks and the P–Tr boundary from this and previously published studies. The two vertical, dotted lines represent the age range imposed by U–Pb data for the ash beds immediately above and below the boundary clay layer [8].

Locations of the four samples dated in this study are shown in Fig. 1. U–Pb isotopic data have been obtained for: (1) mela-nephelinite from the Arydzhangsky Suite; (2) trachydacitic lava and trachyrhyodacite tuff from the Delkansky Suite; (3) carbonatite from the Guli intrusive-volcanic complex; and (4) granodiorite from the Bolgokhtokh stock in the Noril'sk area. Previously determined ages from the Siberian flood-volcanic rocks by this and other isotopic methods have been summarized in Fig. 3.

3. Analytical methods

Perovskite was dissolved in a mixture of equal parts of HF and HNO_3 with a mixed ^{205}Pb–^{230}Th–^{235}U tracer solution in Savillex capsules at about 100°C for 3 days, then dried and re-dissolved in a 9 N solution of HBr. Baddeleyite and zircon were dissolved in Teflon dissolution bombs in ~0.20 ml of HF and ~0.02 ml HNO_3 in the presence of a ^{205}Pb–^{235}U spike. U, Th, and Pb were isolated using miniaturized anion-exchange columns [23]. U and Pb were loaded onto outgassed Re filaments with silica gel. Th was loaded onto Re filaments between two layers of colloidal graphite and run as Th^+ [24]. Further procedural details are reported in [25]. Procedural blanks were usually about 1 pg for Pb and 0.1 pg for U and Th; blank isotopic composition is $^{206}Pb/^{204}Pb = 18.22$, $^{207}Pb/^{204}Pb = 15.61$; $^{208}Pb/^{204}Pb = 39.36$ with 1σ errors estimated at 2%. Isotopic ratios were measured on a VG354 mass spectrometer in single-collector mode using a Daly detector and an analog multiplier. This detector had a constant mass-discrimination factor of 0.4%/amu. Some of the perov-

skite ratio determinations were made after the installation of an ion-counting system. This detector system had a mass-discrimination factor of 0.07% and a dead time of 23.0 ns. A thermal, mass-fractionation correction of 0.10%/amu for both Pb and U was used. Corrections for mass fractionation and dead time were determined by measuring the SRM982 Pb standard. Age and error propagation calculations were made using the programs of Ludwig [26] and Davis [27].

4. Results

4.1. Mela-nephelinite from the Arydzhangsky Suite

The Arydzhansky Suite is the lowermost unit in the Kotuy River basin and is correlative with the Ivakinsky Suite of the Noril'sk area (Fig. 2). Our 30 kg mela-nephelinite sample was collected approximately 200 m above the base of the suite, near the location of the sample studied by [4]. In detail, the sample is equivalent to sample 3FG-9 of ([14], their table 2 and figure 6) and was collected along traverse 1 (their figure 5). Perovskite ($CaTiO_3$) recovered from this rock occurs as small (50–200 μm), dark brown, octahedra and crystal fragments. This mineral appears to be a useful geochronometer for dating alkaline volcanic rocks, as it contains adequate concentrations of U (30–89 ppm) and Th (600 to >2000 ppm). It also contains appreciable amounts of common Pb, making an age determination sensitive to the isotopic composition of the common Pb correction. In this study, the initial Pb isotopic composition in perovskite was estimated by measuring the Pb isotopic composition of two fractions of co-magmatic clinopyroxene (average $^{206}Pb/^{204}Pb = 18.22 \pm 0.06$; $^{207}Pb/^{204}Pb = 15.503 \pm 0.048$; $^{208}Pb/^{204}Pb = 38.20 \pm 0.28$). Values for each fraction were corrected for slight in-growth of radiogenic Pb using the measured $^{238}U/^{204}Pb$ ratios of 11.71 ± 0.08 and 12.89 ± 0.12 (2σ). A whole-rock isotopic composition was not determined, due to the presence of carbonate minerals (calcite and strontianite) of uncertain origin. Uncertainty in the initial Pb correction is numerically propagated through the error calculation. Thirteen concordant and overlapping data points give a weighted mean $^{206}Pb/^{238}U$ age of 251.7 ± 0.4 Ma (MSWD = 0.52; Fig. 4A and Table 1). This age is slightly younger than the 252.1 ± 0.4 Ma age previously reported [7], due to the determination of an improved initial Pb isotopic composition based on clinopyroxene rather than carbonate. Given that the $^{206}Pb/^{204}Pb$ ratios for perovskite vary from 37.4 to 48.8, the proportion of the common Pb correction is about 50% for $^{206}Pb/^{238}U$ and extends to 94% for $^{207}Pb/^{235}U$; hence, the $^{207}Pb/^{235}U$ age is quite imprecise.

The three-dimensional linear isochron is an alternative data-treatment method [26] that gives the age for a closed U–Pb system with an unknown, initial common Pb composition. This tests for both concordance and the assumption of an invariant common Pb composition. The projection of data that represent the 13 perovskite and the two clinopyroxene fractions is concordant and has an intercept age of 251.7 ± 0.9 Ma (MSWD = 4.9), identical to the $^{206}Pb/^{238}U$ weighted mean age. The MSWD is high because the two common Pb measurements on the clinopyroxene do not overlap within error, possibly because their analytical errors are underestimated. The high age precision is due to the spread in Pb afforded by the clinopyroxene data, which plot very near the common Pb plane. If the data for the 13 perovskite fractions are regressed without the clinopyroxene, the age remains the same but the error is larger at 251.7 ± 2.5 Ma (MSWD = 1.2). The initial common Pb composition, indicated by the projection of this isochron, is $^{206}Pb/^{204}Pb = 18.22 \pm 0.26$ and $^{207}Pb/^{204}Pb = 15.494 \pm 0.018$, within error of the measured clinopyroxene initial Pb, which suggests that the correct common Pb composition was used in the weighted mean $^{206}Pb/^{238}U$ age calculation.

The Th–Pb data are more variable than the $^{206}Pb/^{238}U$ data. The weighted mean $^{208}Pb/^{232}Th$ age is 249.9 ± 0.8 Ma but with an MSWD of 3.8. The $^{232}Th/^{204}Pb$ versus $^{208}Pb/^{204}Pb$ isochron age of 247.6 ± 3.6 Ma (MSWD = 2.7) is less sensitive to recent disturbance but also less precise. These ages are calculated with the accepted ^{232}Th decay constant of 4.948×10^{-11} of [28]. If re-calculated with the decay constant of 4.934×10^{-11} reported

Table 1
U–Th–Pb isotopic data for perovskite from mela-nephelinite of the Arydzhangsky Suite

No.	Weight	U	Th	Th/U	PbC	Atomic ratios																Ages (Ma)			
	(mg)	(ppm)	(ppm)		(ppm)	$^{206}Pb/^{204}Pb$	2σ (%)	$^{207}Pb/^{204}Pb$	2σ (%)	$^{208}Pb/^{204}Pb$	2σ (%)	$^{232}Th/^{204}Pb$	2σ (%)	$^{206}Pb/^{238}U$	2σ (%)	$^{207}Pb/^{235}U$	2σ (%)	$^{207}Pb/^{206}Pb$	2σ (%)	$^{208}Pb/^{232}Th$	2σ (%)	$^{206}Pb/^{238}U$	2σ abs	$^{208}Pb/^{232}Th$	2σ abs
1	0.106	77	1467	19.0	6.4	48.8	0.41	17.1	0.44	226	0.46	15 044	0.67	0.03986	0.55	0.2853	5.3	0.0519	5.0	0.012490	0.53	252.0	1.4	250.9	1.3
2	0.254	77	1701	22.2	7.0	45.7	0.36	16.9	0.41	237	0.41	15 863	0.56	0.03987	0.54	0.2870	5.5	0.0522	5.2	0.012556	0.48	252.0	1.3	252.2	1.2
3	0.034	49	1995	41.0	6.4	37.4	0.40	16.5	0.24	294	0.70	20 388	0.97	0.03981	0.62	0.2867	5.9	0.0522	5.6	0.012530	0.75	251.6	1.5	251.7	1.9
4	0.039	80	1878	23.4	8.2	42.9	0.32	16.8	0.22	224	0.45	14 978	0.64	0.03988	0.49	0.2816	4.5	0.0512	4.3	0.012435	0.45	252.1	1.2	249.8	1.1
5	0.054	89	1724	19.3	7.9	46.8	0.31	16.9	0.26	216	0.40	14 300	0.75	0.03986	0.48	0.2753	4.3	0.0501	4.0	0.012422	0.66	252.0	1.2	249.5	1.6
6	0.053	82	1731	21.1	7.7	45.1	0.28	16.9	0.22	221	0.38	14 684	0.56	0.03983	0.57	0.2856	4.1	0.0520	3.8	0.012440	0.43	251.8	1.4	249.9	1.1
7	0.038	85	1558	18.3	7.3	47.3	0.35	17.0	0.18	210	0.48	13 836	0.67	0.03977	0.69	0.2811	3.7	0.0513	3.4	0.012452	0.44	251.4	1.7	250.1	1.1
8	0.060	81	1749	21.5	7.3	46.0	0.23	16.9	0.16	231	0.34	15 529	0.52	0.03970	0.44	0.2772	3.8	0.0506	3.5	0.012430	0.43	251.0	1.1	249.7	1.1
9	0.042	78	1792	22.8	7.7	43.6	0.29	16.8	0.17	226	0.42	15 076	0.73	0.03977	1.48	0.2805	4.3	0.0511	3.9	0.012467	0.59	251.4	3.7	250.4	1.5
10[a]	0.062	30	1214	40.7	3.7	38.2	0.38	16.5	0.22	299	0.60	21 158	0.80	0.03974	0.53	0.2685	5.8	0.0490	5.5	0.012328	0.47	251.2	1.3	247.6	1.2
11[a]	0.023	47	607	12.8	4.9	42.2	0.79	16.7	0.31	137	0.98	7 992	1.47	0.03986	0.72	0.2690	5.6	0.0490	5.3	0.012395	0.71	252.0	1.8	249.0	1.8
12[a]	0.011	58	2649	45.3	7.3	38.3	1.26	16.5	0.84	326	1.81	23 474	2.24	0.03998	1.28	0.2764	13.7	0.0501	12.8	0.012265	0.99	252.7	3.2	246.4	2.4
13	0.010	82	1807	22.0	8.4	42.8	1.04	16.7	0.30	213	1.46	14 028	1.96	0.03982	0.97	0.2750	5.2	0.0501	4.8	0.012483	0.83	251.7	2.4	250.8	2.1

Atomic ratios corrected for spike, fractionation, blank and initial common Pb. $^{206}Pb/^{204}Pb$, $^{207}Pb/^{204}Pb$, $^{208}Pb/^{204}Pb$ corrected for spike and fractionation only. Initial common Pb used in age calculation from co-magmatic clinopyroxene ($^{206}Pb/^{204}Pb = 18.22 \pm 0.06$; $^{207}Pb/^{204}Pb = 15.503 \pm 0.048$; $^{208}Pb/^{204}Pb = 38.2 \pm 0.280$).
[a] Single-grain analyses; all fractions air-abraded [73].

in [25], they would be within error of the U–Pb age. It was expected that the Th–Pb system in perovskite would provide a robust geochronometer due to the high Th/U values of 13–45, and the consequently higher proportion of radiogenic ^{208}Pb isotope relative to initial Pb. However, the Th–Pb age is less useful than the U–Pb age due to the large error and possible bias resulting from excess scatter and uncertainty in the ^{232}Th decay constant.

The scatter of Th–Pb data is surprising in view of the coherence of the ^{206}Pb/^{238}U system and the fact that Th should be more chemically immobile than both U and Pb. The radiation damage resulting from the Th–Pb decay chain is less than that from either of the two U–Pb chains. Thus, it seems unlikely that thorogenic ^{208}Pb could be preferentially leached, especially if there is no apparent loss of ^{206}Pb, and no apparent correlation between ^{208}Pb/^{232}Th and ^{206}Pb/^{238}U ages. Two possible explanations are that there are residual altered domains, which lost almost all of the original U and radiogenic Pb, but retained Th, or that the mineral contains zones with distinctly higher Th/U ratios that became damaged and preferentially lost Pb. The first alternative seems most likely. Minerals rich in Th such as monazite have been found in zircon alteration assemblages, probably because Th acts as an immobile element during mineral alteration. The deeply colored to opaque nature of perovskite makes it difficult to check for alteration along cracks. Loss of both U and Pb would leave the U–Pb ages unaffected, but retention of Th would appear as a Th gain, which lowers the age similarly to a loss of ^{208}Pb. In this case, the oldest ^{208}Pb/^{232}Th ages should be closest to the age of crystallization. The two oldest ages are within error of each other and give a weighted mean of 252.1 ± 1.0 Ma. This is within analytical error of the 251.7 ± 0.4 Ma mean ^{206}Pb/^{238}U age and is well within error when the ca. ± 0.2% uncertainties in the ^{238}U and ^{232}Th decay constants are included.

A small population of xenocrystic zircons was recovered from this sample. They are small, generally euhedral, colorless crystals weighing from less than 1 μg to several μg. Four grains give near-concordant data, with ^{206}Pb/^{238}U ages of 362.3 ± 4.4, 364.6 ± 3.8, 409.9 ± 1.8, and 493.8 ± 4.4 Ma, and one imprecise, discordant data point has a ^{206}Pb/^{238}U age of 386.4 ± 9.6 Ma and a ^{207}Pb/^{235}U age of 489.2 ± 65.4 Ma (Fig. 4B). These zircons apparently reflect entrainment of material during passage through pre-Carboniferous basement.

4.2. *Trachydacite and trachyrhyodacite from the Delkansky Suite*

Ages for trachydacitic lava (2FG-58 of [12], their figure 5 and table 2) and trachyrhyodacite tuff (1FG-229) from the middle of the Delkansky Suite of the Maymecha River basin, situated

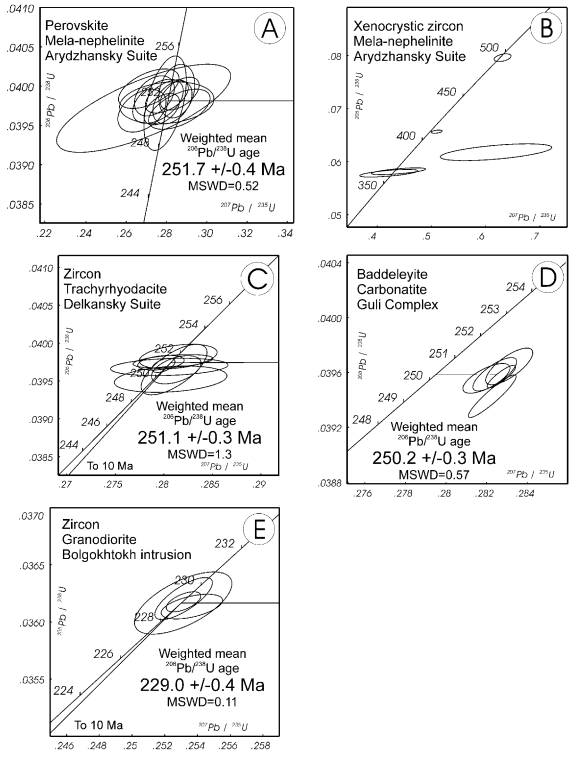

Fig. 4. Concordia diagrams showing data for (A) perovskite from mela-nephelinite of the Arydzhangsky Suite, Maymecha–Kotuy area, (B) single, xenocrystic zircons from mela-nephelinite of the Arydzhangsky Suite, Maymecha–Kotuy area, (C) zircon from trachydacite and trachyrhyodacite of the Delkansky Suite, Maymecha–Kotuy area, (D) baddeleyite from carbonatite of the Guli Complex, Maymecha-Kotuy area, (E) zircon from granodiorite of the Bolgokhtokh intrusion, Noril'sk area.

stratigraphically ~2000 m above the Arydzhangsky mela-nephelinite, provide a time estimate for the waning stages of Siberian flood volcanism, as the Delkansky Suite lavas are interpreted to be considerably younger than any in the Noril'sk area [12]. Eruption of the overlying 1400 m thickness of meymechitic lavas appears to have been extremely rapid, as there are few distinct flow boundaries. Fedorenko and Czamanske [12] concluded that the meymechitic lava pile effectively cooled as a unit. The two samples (28 kg total weight) were collected from the same stratigraphic level in the Delkansky Suite, 2FG-58 in the middle of traverse 9 and 1FG-229 in the middle of traverse 10 of figure 4 in [12]. Zircons are pale brown to colorless, euhedral, short prismatic, doubly terminated crystals. U–Pb isotopic data obtained from each sample are analytically indistinguishable and so were pooled to yield one age. Eight concordant and overlapping data points obtained from multigrain and one single-grain fraction give a weighted mean $^{206}Pb/^{238}U$ age of 251.07 ± 0.36 Ma (MSWD = 1.3; Fig. 4C and Table 2). If the youngest $^{206}Pb/^{238}U$ age of 249.88 ± 1.08 Ma is removed from the weighted mean age calculation, an age of 251.14 ± 0.27 Ma (MSWD = 0.56) is obtained. The concordia age [29] is identical at 251.08 ± 0.26 Ma (MSWD of concordance and equivalence is 0.86, probability is 0.61). The pooled age for these two Delkansky-Suite samples establishes a younger limit for the time of a magnetic reversal between deposition of normally polarized Onkuchaksky Suite lavas and those of the overlying, reversely polarized Tyvankitsky Suite, which lies immediately below the Delkansky Suite.

4.3. *Carbonatite from the Guli intrusive-volcanic complex*

The Guli intrusive-volcanic complex, exposed over ~2000 km^2, is composed largely of ultramafic and alkaline rocks, and hosts two late carbonatite stocks ([12] and references therein). The Guli intrusion clearly cuts the Onkuchaksky and Tyvankitsky suites, but contacts with the Delkansky and Maymechinsky suites are not exposed. The intrusion is contiguous with Maymechinsky Suite exposures and the three early phases of the intrusion (dunite–peridotite, ankaratrite, and ijolite–melteigite) are similar to meymechite in geochemistry. Thus, one may conclude that undifferentiated meymechite magmas were erupted, followed by differentiated remains of this magma, to produce the early phases of the Guli intrusion. Our 20 kg sample is a calcitic carbonatite, collected from the north part of the most southerly carbonatite in the complex. Baddeleyite (ZrO_2) extracted from this carbonatite forms clear, dark brown, equant fragments. Four single fragments give overlapping data with a weighted mean $^{206}Pb/^{238}U$ age of 250.2 ± 0.3 Ma (MSWD = 0.57; Fig. 4D and Table 2), which form a tight cluster that plots distinctly to the right of the concordia curve. A fifth datum plots slightly below the cluster and is excluded from the final age calculation. These data are discordant, and give distinctly older, weighted mean $^{207}Pb/^{235}U$ and $^{207}Pb/^{206}Pb$ ages of 252.7 ± 0.3 and 278 ± 4 Ma, respectively. The intrusive relation of this carbonatite to the Guli complex and the volcanic pile, and the age of the Delkansky samples presented above, eliminate the possibility that the $^{207}Pb/^{235}U$ and $^{207}Pb/^{206}Pb$ ages are geologically meaningful. The common Pb correction cannot be a factor in explaining these data because the $^{206}Pb/^{204}Pb$ ratios are high, ranging from 2230 to 17 850. These results may indicate the presence of unsupported, excess ^{207}Pb due to the presence of ^{231}Pa in excess of radioactive equilibrium. ^{231}Pa is the only relatively long-lived (half-life of 32 400 yr), intermediate nuclide in the ^{235}U decay chain. If this explanation is valid, a high $^{231}Pa/^{235}U$ ratio in the melt may be responsible. Examples of unsupported ^{207}Pb have been reported by [25,30,31], who also ascribed it to excess ^{231}Pa. The pattern of excess ^{207}Pb-induced discordance reported here is similar to that reported by [25] for baddeleyite from carbonatite. Anczkiewicz et al. [30] and Mattinson [31] found a distinctly different discordance pattern for zircon data from pegmatite, which produced a horizontal array with uniform $^{206}Pb/^{238}U$ ages and variable $^{207}Pb/^{235}U$ ages. This suggests that the pegmatite zircons crystallized from a fluid with rapidly changing Pa/U ratios, which is in contrast to the carbonatite melt that would have

Table 2
U–Pb zircon and baddeleyite data for volcanic rocks, carbonatite, and granodiorite units from the Siberian Flood-Volcanic Province, Russia

# grains	Weight (mg)	U (ppm)	Th/U	PbC (pg)	$^{206}Pb/^{204}Pb$	$^{206}Pb/^{238}U$	2σ	$^{207}Pb/^{235}U$	2σ	$^{207}Pb/^{206}Pb$	2σ	Age (Ma) $^{206}Pb/^{238}U$	2σ	Age (Ma) $^{207}Pb/^{235}U$	2σ	% Disc.
Trachyrhyodacite																
8 zircons	0.011	41	1.08	0.9	1 305	0.03982	0.00016	0.2815	0.0040	0.05127	0.00069	251.7	1.0	251.8	3.2	0.4
7 zircons	0.007	93	1.01	1.0	1 632	0.03976	0.00009	0.2810	0.0041	0.05125	0.00071	251.3	0.5	251.4	3.3	0.3
15 zircons[a]	0.027	68	0.99	1.8	2 618	0.03974	0.00010	0.2797	0.0024	0.05105	0.00041	251.2	0.6	250.4	1.9	−3.5
15 zircons[a]	0.035	59	1.06	1.1	4 852	0.03971	0.00009	0.2800	0.0012	0.05114	0.00019	251.0	0.6	250.6	1.0	−1.6
10 zircons[a]	0.018	61	1.00	4.2	683	0.03969	0.00011	0.2806	0.0061	0.05128	0.00108	250.9	0.7	251.1	4.8	0.9
7 zircons[a]	0.010	80	1.07	0.9	2 319	0.03965	0.00019	0.2813	0.0026	0.05146	0.00042	250.6	1.2	251.7	2.0	4.2
1 zircon	0.003	139	0.91	0.6	1 696	0.03965	0.00033	0.2811	0.0034	0.05141	0.00045	250.7	2.1	251.5	2.7	3.4
2 zircons[a]	0.010	78	0.96	2.3	882	0.03952	0.00017	0.2807	0.0058	0.05151	0.00103	249.9	1.1	251.2	4.6	5.3
Carbonatite																
1 baddeleyite	0.005	525	0.08	1.2	5 454	0.03964	0.00013	0.2831	0.0012	0.05179	0.00014	250.6	0.8	253.1	0.9	9.5
1 baddeleyite	0.004	782	0.11	1.2	6 511	0.03959	0.00010	0.2824	0.0011	0.05173	0.00014	250.3	0.6	252.6	0.9	8.7
1 baddeleyite	0.002	1605	0.12	1.6	5 083	0.03956	0.00011	0.2820	0.0012	0.05170	0.00015	250.1	0.7	252.2	0.9	8.2
1 baddeleyite	0.006	1269	0.21	1.1	17 666	0.03955	0.00009	0.2825	0.0008	0.05181	0.00010	250.0	0.5	252.6	0.6	9.9
1 baddeleyite	0.005	1130.3	0.20	1.1	13 296	0.03943	0.00016	0.2823	0.0012	0.051925	0.00008	249.3	1.0	252.5	0.9	11.9
Granodiorite																
1 zircon	0.002	648	0.76	1.0	3 116	0.03621	0.00018	0.2532	0.0018	0.05071	0.00023	229.3	1.1	229.1	1.4	−0.7
1 zircon	0.002	415	0.78	1.1	1 828	0.03617	0.00027	0.2531	0.0030	0.05076	0.00047	229.0	1.7	229.1	2.4	0.5
8 zircons	0.014	332	0.80	2.8	3 930	0.03616	0.00008	0.2531	0.0011	0.05077	0.00018	229.0	0.5	229.1	0.9	0.6
4 zircons	0.008	422	0.74	1.8	4 336	0.03614	0.00011	0.2537	0.0011	0.05090	0.00020	228.9	0.7	229.5	0.9	3.2
Arydzhansky mela-nephelinite																
1 zircon	< 0.001	65	0.66	1.2	120.2	0.05781	0.00071	0.421	0.054	0.0528	0.0063	362.3	4.4	356.8	38.6	−13
1 zircon	0.001	46	0.66	1.7	119.6	0.05818	0.00063	0.439	0.050	0.0547	0.0059	364.6	3.9	369.6	35.6	9.4
1 zircon	0.002	104	0.76	1.4	630.0	0.06566	0.00030	0.509	0.010	0.0563	0.0011	409.9	1.8	418.1	6.9	11.9
1 zircon	< 0.001	47	0.64	1.0	71.9	0.06178	0.00158	0.619	0.103	0.0727	0.0112	386.4	9.6	489.2	65.5	63.4
1 zircon	0.003	24	0.62	0.7	521.7	0.07961	0.00073	0.631	0.016	0.0575	0.0013	493.8	4.4	496.7	9.8	3.4

All zircons have been air-abraded [74]; baddeleyite has not been abraded.
Th/U ratio determined from radiogenic $^{208}Pb/^{206}Pb$ ratio and $^{207}Pb/^{206}Pb$ age.
PbC is total common Pb; the total amounts have been assigned the blank isotopic composition.
% Disc. is percent discordant from $^{207}Pb/^{206}Pb$ age assuming zero-age Pb loss.
[a] Analyses are from the same rock sample.

had relatively constant Pa/U ratios, having been fractionated nearer to the source.

4.4. Granodiorite from the Noril'sk area

A late, distinct phase of magmatism in the Noril'sk area is recorded by the intrusion of the Bolgokhtokh granodioritic stock. Zircon analyses give concordant data, with weighted mean $^{206}Pb/^{238}U$ and $^{207}Pb/^{235}U$ ages of 229.0 ± 0.4 (MSWD = 0.11) and 229.3 ± 0.5 Ma (MSWD = 0.19), respectively (Fig. 4E and Table 2). The concordia age is 229.05 ± 0.36 Ma (MSWD of concordance and equivalence is 0.41, probability is 0.90).

5. Discussion

5.1. Temporal framework of the Siberian flood-volcanic event and later magmatism and its implications

The perovskite age of 251.7 ± 0.4 Ma, presented here for the 350 m thick, melilite-bearing, melanephelinitic to limburgitic rocks of the Arydzhansky Suite [14] is interpreted to represent the time of onset of Siberian flood volcanism. The zircon age for trachydacitic and trachyrhyodacitic samples from the Delkansky Suite in the upper part of this volcanic sequence establishes a maximum age for cessation of volcanism at 251.1 ± 0.3 Ma. This is a maximum age because ~1400 m of high-Ti, Mg-rich lava of the Meymechinsky Suite lies above the Delkansky Suite, and may represent a few hundred thousand years of eruptive activity. This age is well within error of the 251.2 ± 0.3 Ma age obtained for the Noril'sk I intrusion [6] and supports numerous previous suggestions that these mineralized intrusions are co-magmatic with volcanism. Stratigraphic correlation with the volcanic sequence at Noril'sk indicates that the thickness of the volcanic sequence bracketed by the Arydzhansky and Delkansky Suite samples is about 5000 m, extruded over a period of ~0.6 Myr. This was followed ~1 Myr later at 250.2 ± 0.3 Ma with the intrusion of carbonatite which cuts the Guli intrusive-volcanic complex.

Previous arguments for a short duration of volcanism had been based on consideration of the errors associated with $^{40}Ar/^{39}Ar$ dating of a limited sample suite [1] and on comparison of paleomagnetic data for samples from the Noril'sk area with the perceived magnetostratigraphy of the period [13]. The most conservative interpretation of the present results sets a time span of 251.7 ± 0.4 Ma to 251.1 ± 0.3 Ma (0.6 ± 0.6 Myr) for eruption of the bulk of the flood-volcanic rocks.

Our dated samples likely encompass most of the duration of Siberian flood magmatism. The Ivakinsky Suite of the Noril'sk area could be slightly older than the Arydzhangsky Suite of the Maymecha–Kotuy area, but the difference is likely to be minor because both sequences lie disconformably upon Permian coal-bearing sediments and therefore represent the first outpourings of lava in each area. Six types of mafic intrusions are known in the Noril'sk area to post-date volcanic eruption (e.g. [32]). However, four of them are geochemically similar to, and likely coeval with, the lavas of the Maymecha–Kotuy area [12]. It is uncertain whether the type-7 trachydolerite dikes, which cut the entire Maymechinsky Suite in the Maymecha–Kotuy area, could be younger than the Guli intrusive-volcanic complex.

About 21 Myr following the cessation of volcanic activity, minor silicic intrusive activity is represented by emplacement of the Bolgokhtokh granodioritic stock at 229.0 ± 0.4 Ma. This age is older than the $^{40}Ar/^{39}Ar$ age of 223 ± 1 Ma reported by [3], which was based on well-defined, incremental-heating plateaus for fresh biotite from two samples separated by 100 m in drill core, as well as consistent total-fusion ages for coexisting hornblende. No explanation can readily be suggested for the discrepancy. This stock represents the youngest recorded magmatic pulse in the Noril'sk area, and may be related to Late Triassic tectogenesis which shaped the present structural plan of the northern Siberian Platform. Based on chemical and isotopic data, Wooden et al. [33] suggested that the granodiorite formed by melting of lower crust.

High eruption rates (0.5–1 km^3/yr) of enormous volumes of magma have been cited as supporting evidence for a plume origin for large igneous

provinces, including the Deccan, Parana, Karoo, North Atlantic Tertiary, and Columbia River flood basalts. In each case, the major volume of lava appears to have been erupted over a very short time interval (1–2 Myr), with volcanic or intrusive activity possibly continuing at a greatly reduced rate (e.g. [34]). The plume model predicts large-scale crustal uplift, with rapid and voluminous flood-basalt eruptions and hotspot tracks, caused by decompression melting in response to the arrival of a large plume head followed by a narrow tail. Based on numerical modeling, Farneti and Richards [35] estimated that a plume head with a 400 km radius would cause crustal uplift of 2–4 km sustained for 5–20 Myr over the broad area occupied by the Siberian flood-volcanic rocks.

A plume-model origin has frequently been invoked for the Siberian traps (e.g. [1,4,33,36]); however, this is in conflict with geologic evidence. The Siberian lavas are underlain everywhere by rhythmically alternating terrigenous sedimentary rocks of the Tungusskaya Series [37]. The Tungusskaya Series, Middle Carboniferous (~320 Ma) to Late Permian (~250 Ma) in age, varies in thickness from 100–150 to 1400 m. It includes the Tungusskaya coaliferous basin, which contains 24 coal beds and is considered to represent the largest coal basin in the world [38]. There is only minor disconformity between the underlying sedimentary rocks and the lavas. Contact relations between the lava flows show that the volcanic pile accumulated in an area of low relief that became somewhat more elevated with time (evolving from subaqueous to subaerial) in both the Noril'sk and Maymecha–Kotuy areas. Hence, both the Tungusskaya sediments and the lavas accumulated in an environment of mild but continuous subsidence, balanced by sedimentation and deposition of volcanic rocks [37]. Models that account for massive basaltic magmatism without surface uplift have been presented [39–41].

5.2. *Timing of Siberian flood volcanism relative to the Permo–Triassic boundary event*

Unlike the Cretaceous–Tertiary (K–T) boundary clay layer (e.g. [42,43]) that has been shown conclusively to contain fallout caused by the impact of a large comet or meteorite that formed the Chicxulub crater on the Yucatan peninsula (e.g. [44–47]), the Permian–Triassic (P–Tr) boundary layers have so far revealed only limited, unconfirmed reports of an extraterrestrial impact. A recent report of fullerenes containing extraterrestrial noble gases in P–Tr boundary sediments from the Meishan section, Zhejiang Province, SE China, and the Sasayama section in Japan may be the first evidence for impact thus far reported [48]. However, this finding remains controversial, as attempts to reproduce these results have failed [49], and both the boundary units studied and the analytical methods used by Becker et al. have been questioned [50–52]. Kaiho et al. [53] present isotopic and geochemical data obtained from two boundary clay layers at the same locality. They report light $\delta^{34}S$ values, a negative Sr excursion, and the presence of Fe–Si–Ni fragments. Despite the equivocal significance of these data, Kaiho et al. concluded that a meteorite impact was responsible for the mass extinction event (cf. [54]). A comprehensive review of this and other extinction hypotheses is given in [55].

For volcanism to have triggered a devastating mass-extinction event it must be shown that it both coincides with (or slightly predates) the event, and that it occurred over a geologic time interval brief enough to overwhelm atmospheric and biospheric systems. Renne et al. [4] were the first to use high-precision ages to demonstrate a temporal linkage between the two events. They applied precise $^{40}Ar/^{39}Ar$ methods to feldspars from tuffs near the P–Tr boundary at Meishan (bed 25) and determined a weighted mean age of 250 ± 1.5 Ma. This agrees within error with a recalculated age of 249.6 ± 1.5 Ma [4] originally determined on plagioclase and whole rocks from lavas of the basal Ivakinsky Suite at Noril'sk [1]. The small, systematic discrepancy between ages determined by U–Pb and Ar/Ar may in part be related to errors in the decay constants, especially that for ^{40}K, which is less precisely determined than that for ^{238}U (e.g. [56]).

The U–Pb ages from this study are the first to directly constrain the extremely short duration of Siberian flood volcanism and thus lend further

credence to the idea of a causal link between this volcanism and the P–Tr extinctions. There is a remarkable correlation between the U–Pb age of 251.7 ± 0.4 Ma reported here for the initiation of flood volcanism, the age of 251.4 ± 0.3 Ma [8] for the P–Tr boundary, and the age of 251.2 ± 0.3 Ma [6] for emplacement of the Noril'sk I intrusion.

The U–Pb zircon age presented by [8] is based on the study of six ash beds sampled in quarry A near Meishan, Zhejiang Province, southern China. Most relevant are the ages obtained for bed 25, the 'boundary ash' (MAW-b25, located about 18 cm below the paleontologically defined P–Tr boundary), and the layers just below [bed 20, MZ96-(−4.3)] and above the ash [bed 28, MZ96-(+0.17)]. Concordant data for single- and multi-grain analyses led to estimates of 252.3 ± 0.3 and 250.7 ± 0.3 Ma, respectively, for beds 20 and 28. An apparent bimodal age population was found for the boundary ash itself, one cluster of concordant data giving an age of ~252.7 ± 0.4 Ma, the other, an age of 251.4 ± 0.3 Ma. In light of the constraint imposed by their age for bed 20, Bowring et al. interpreted the older age obtained for the boundary ash to inheritance of slightly older xenocrysts, and interpreted the age of 251.4 ± 0.3 Ma as the best estimate for the P–Tr stratigraphic boundary. The weighted mean $^{206}Pb/^{238}U$ ages obtained by [8] for beds 20 and 28 are represented by vertical dotted lines in Fig. 3. These beds bracket the P–Tr boundary. Their ages also bracket the Siberian flood-volcanic event and are within error of the ages obtained for the upper and lowermost dated units of the volcanic sequence. Bowring et al. also presented a similar age for ash collected 100 km away at Penglaitan, for which the conodont control is now established.

A contrasting interpretation was given by [57], who reported U–Pb zircon IDTIMS ages on single zircons for ash layers near the P–Tr boundary zone, as well as from the boundary ash sample that is reported to be stratigraphically equivalent to the one studied by [8]. Their data on 19 individual zircons from the boundary ash show a spread in $^{206}Pb/^{238}U$ ages from which no single, coherent age could be interpreted. The dispersion of their results was attributed to Pb loss, minor amounts of inheritance, and/or the presence of slightly older xenocrystic grains. However, zircons from an ash layer located 8 cm above the boundary ash yielded six reproducible data, with a weighted mean $^{206}Pb/^{238}U$ age of 252.5 ± 0.3 Ma. On this basis, [57] concluded that the P–Tr boundary must be older. If our ages for Siberian flood volcanism are correct, the age obtained by [57] for the boundary would imply that the mass-extinction event pre-dated volcanism by a small but resolvable interval and that the two events are unrelated.

The reason for the discrepancy in the ages obtained by [8] and [57] remains to be understood. The only significant difference between the methods of the two studies was the application of a hot (80°C) hydrofluoric/nitric acid pre-treatment of the zircons in the study by [57]. Mattinson [58] suggested that this procedure has the potential to fractionate U and Pb, although such an effect is not extensively documented. It is also possible that the zircons dated by [57] at 252.5 ± 0.3 Ma from above the boundary were inherited from slightly older parts of the volcanic edifice that formed the source of the ash layer. Mundil et al. also obtained an age of 252.0 ± 0.4 Ma on a coherent data set of 10 analyses from a unit 17.3 m below the boundary, which, if stratigraphically reliable, would place a maximum age on the extinctions in agreement with our results and those of [8]. If the Mundil et al. interpretation is correct, data from both [8] and our study must be similarly affected by Pb loss resulting in ages that are too young. This seems unlikely because it would require (1) that the degree of Pb loss be uniform enough not to disturb coherency of multiple analyses, and (2) that it fortuitously resulted in similar ages for multiple samples from Siberia and China. Mundil et al. showed that data obtained from multiple-grain analyses can produce tight clusters of data with biased ages from Pb loss or inheritance. Multiple-grain analyses give data with greater precision, enabling a stricter test on coherency, but errors do not go down proportionately, so the averaging effect would dominate. However, some of our analyses contain only one or two grains and data for these are in agreement with the mean. Also, Pb from our larger fractions is

more radiogenic, making it less susceptible to common Pb corrections, which could bias the age of smaller single-grain samples. Carrying out single-grain analysis is preferable in future studies, but will require higher levels of precision and sensitivity. For presently available data, the mutual agreement and coherence of ages from several samples (three from Siberia and three from China) is a strong argument that the measured ages represent coherent stratigraphic events and are probably accurate to within the error of their means.

5.3. Evidence of environmental effects

The nature and proposed mechanisms of extinction at the P–Tr boundary have been extensively reviewed [55]. Climatic effects related to global warming are strongly implicated. There is good evidence for anomalously high CO_2 levels (e.g. [59]) and marine anoxia [60]. Although gas contents of basalts are variable, eruption of 2×10^6 km^3 of basalt could release 4×10^{19} g of CO_2 and over 10^{19} g of SO_2, based on estimates from Kilauea volcano [61,62]. The CO_2 emission is about 15 times the content of the present atmosphere. Excess atmospheric CO_2 would be buffered through the weathering cycle over a 100 kyr time scale [63], but if released over 600 kyr or less this should leave an imprint in the rock record and produce a short-term increase in global temperatures. Combined with rainout of H_2SO_3 and other acids, the increased atmospheric CO_2 would also cause intense weathering. Evidence for this is found in paleosol claystone breccias from widely separated localities at the P–Tr boundary [64], which show evidence of extreme leaching of alkaline and alkaline earth elements.

Rapid release of extensive quantities of deleterious gases is evident from persistent tuffaceous units (>10 m thick) that occur frequently throughout the Noril'sk-area lava sequence (e.g. see figure 2 of [33]) and on the Putorana plateau (see figure 1 in [12]), where even thicker tuff units are present. If the correlations indicated in Fig. 2A are accurate, consideration of the age of the Noril'sk I intrusion within the context of the ages herein reported for the Maymecha–Kotuy sequence suggests that a substantial portion of the Siberian flood-volcanic province may have been erupted in only $\sim$0.1 Myr, dramatically increasing the atmospheric burden.

Sufficiently rapid release of large quantities of CO_2 from volcanism would flood the exogenic system with mantle-derived CO_2 having a carbon isotopic composition ($\delta^{13}C$) of -4. This would have the effect of lowering the $\delta^{13}C$ value of carbonates. Carbonates at the P–Tr boundary show an abrupt lowering of $\delta^{13}C$ from about +2 to -2 [55,65]. The likely amount of volcanically released CO_2 represents only a fifth of the carbon reservoir in the ocean–atmosphere system and is not by itself sufficient to explain the observed carbon isotopic shifts. However, secondary effects of climate warming and sea-level regression leading to clathrate destabilization in the polar regions could greatly enhance atmospheric CO_2 content and carbon isotopic effects [8,66–68]. Isotopes of carbon in methane ice (clathrate) have $\delta^{13}C$ values of about -60 and there is more than enough carbon (10^{19} g) within present oceanic sediments to explain the observed isotopic shifts. Clathrate destabilization at the P–Tr boundary due to ocean warming was also suggested by Krull and Retallack [68] who measured negative $\delta^{13}C$ excursions much lower than mantle $\delta^{13}C$ values in paleosol carbon from P–Tr boundary sections. Thus, the rapid, episodic release of mantle CO_2 from the Siberian flood-volcanic rocks might have driven positive feedback mechanisms that greatly enhanced CO_2 and climatic effects.

In the alpine P–Tr boundary carbonate from Gartnerkofel, $\delta^{13}C$ values fluctuate over a 50 m section, coincident with extinction. Rampino et al. [69] attempted to estimate a sedimentation rate, and therefore the time scale of these fluctuations, by correlating density and γ-ray logs with orbital Milankovitch cycles. Although controversial, their analysis gave an average depositional rate of about 10 cm/kyr. Such a rate yields a time span of 500 kyr over the section recording carbon isotopic fluctuation, comparable with our new geochronological constraints on the duration of flood volcanism. The initial and most profound $\delta^{13}C$ shift apparently occurred over a much shorter

time (< 30–40 kyr), while faunal extinction may have occurred over < 60 kyr [69,70]. The $\delta^{13}C$ core record indicates partial recovery after about 200 kyr, followed by more fluctuations until stabilizing in the lower Triassic. This may record the environmental effects of episodic, increased eruption rates that fed higher parts of the volcanic section.

The preferential extinction of organisms most susceptible to high CO_2 levels (hypercapnia) has been noted by Knoll et al. [71] as evidence for high CO_2 levels at the P–Tr transition. They proposed overturn of anoxic deep ocean water as the cause of extinction. If this occurred, it was likely an additional, secondary environmental effect of volcanism. Given that the age of Siberian flood volcanism appears to be precisely correlated with the extinction event, and its eruption rate appears to have been high enough to overwhelm exogenic CO_2 reservoirs, intense volcanism must be considered the primary cause of extinction at the P–Tr boundary.

Reviews of possible scenarios relating Siberian flood volcanism and the P–Tr boundary mass-extinction event have been presented [8,55,72]. In arguing for a connection between Siberian flood volcanism and the extinctions, Campbell et al. [2] noted several unique features that would have been especially destabilizing to the environment: (1) it appears to represent the largest subaerial volcanic event in the Phanerozoic record; (2) the magmas ascended through a ~5.5 km sedimentary sequence now characterized by abundant anhydrite (e.g. figure 4 in [73]), a potential source of SO_2 in addition to that contained in the magmas from depth; (3) atypically, the volcanic sequence contains ~20% by volume of pyroclastic material, eruption of which would have been accompanied by almost complete release of contained gases; (4) abundant lithic fragments in the tuffaceous rocks attest to the violence of these eruptions (rare fragments from 10 km depth); and (5) the Tungusskaya Series immediately underlying the volcanic sequence contains the world's largest coal basin [37,38]. Thus, much carbonaceous material may have been blasted into the atmosphere, helping to account for the notable $\delta^{13}C$ excursion (e.g. [59]).

6. Conclusions

1. Siberian flood volcanism occurred over a very brief span of geological time. It was initiated at 251.7 ± 0.4 Ma and approached its waning stages at 251.1 ± 0.3 Ma. Major volcanism had terminated by 250.2 ± 0.3 Ma, as established by emplacement of carbonatite which cuts the Guli intrusive-volcanic complex.
2. The coincidence of ages that bracket the volcanic event with those that bracket the age of the Permian–Triassic boundary ash strongly supports arguments that Siberian flood volcanism was a major cause of the biological extinction that defines the end of the Permian period.
3. Extrusion of $2–4 \times 10^6$ km^3 of volcanic material in such a brief geologic time interval (~0.6 Myr) would have released sufficiently large quantities of CO_2, SO_2, fluorine, and chlorine rapidly enough to wreak destruction on atmospheric and biospheric systems.
4. Together with the zircon and baddeleyite age of 251.2 ± 0.3 Ma reported for the Noril'sk I intrusion [6], the results of this study support a genetic relation between the Cu–Ni–PGE-rich intrusions of the Noril'sk–Talnakh area and Siberian flood volcanism.
5. The Bolgokhtokh granodioritic stock of the Noril'sk area was intruded in the Late Triassic at 229.0 ± 0.4 Ma and may mark a later tectonic re-activation that had no relation to the flood-volcanic activity.
6. U–Pb dating of perovskite is a potentially valuable tool for obtaining ages of alkaline volcanic rocks.

Acknowledgements

This study was supported by an NSERC Major Facilities Access grant to T.E. Krogh. Contributive comments from journal reviewers R. Mundil and one anonymous reviewer helped to improve the manuscript and are appreciated. Constructive criticism from F. Corfu on an early version of the manuscript is gratefully acknowledged, as is the

ongoing, co-operative effort of the personnel at the ROM laboratory, and the beneficial advice provided by Tom Krogh. *[BOYLE]*

References

[1] P.R. Renne, A.R. Basu, Rapid eruption of the Siberian Traps flood basalts at the Permo-Triassic Boundary, Science 253 (1991) 176–179.

[2] I.H. Campbell, G.K. Czamanske, V.A. Fedorenko, R.I. Hill, V. Stepanov, Synchronisn of the Siberian Traps and the Permian-Triassic boundary, Science 258 (1992) 1760–1763.

[3] B.G. Dalrymple, G.K. Czamanske, V.A. Fedorenko, O.N. Simonov, M.A. Lanphere, A.P. Likhachev, A reconnaissance $^{40}Ar/^{39}Ar$ geochronological study of ore-bearing and related rocks, Siberian Russia, Geochim. Cosmochim. Acta 59 (1995) 2071–2083.

[4] P.R. Renne, Z. Zichao, M.A. Richards, M.T. Black, A.R. Basu, Synchrony and causal relations between Permian-Triassic boundary crises and Siberian Flood volcanism, Science 269 (1995) 1413–1416.

[5] V.A. Fedorenko, P.C. Lightfoot, A.J. Naldrett, G.K. Czamanske, C.J. Hawkesworth, J.L. Wooden, D.S. Ebel, Petrogenesis of the Flood Basalt Sequence at Noril'sk, North Central Siberia, Int. Geol. Rev. 38 (1996) 99–135.

[6] S.L. Kamo, G.K. Czamanske, T.E. Krogh, A minimum U-Pb age for Siberian flood-basalt volcanism, Geochim. Cosmochim. Acta 60 (1996) 3505–3511.

[7] S.L. Kamo, G.K. Czamanske, Y. Amelin, V.A. Fedorenko, V.R. Trofimov, U-Pb zircon, baddeleyite, and U-Th-Pb perovskite ages for Siberian flood volcanism, Maymecha–Kotuy area, Siberia, Goldschmidt 2000, Oxford, UK, An International Conference for Geochemistry, Eur. Assoc. Geochem. and Geochem. Soc., J. Conf. Abstr. vol. 5, no. 2 (2000) 569.

[8] S.A. Bowring, D.H. Erwin, Y.G. Jin, M.W. Martin, K. Davidek, W. Wang, U/Pb zircon geochronology and tempo of the end-Permian mass extinction, Science 280 (1998) 1039–1045.

[9] M.K. Reichow, A.D. Saunders, R.V. White, M.S. Pringle, A.I. Al'Mukhamedov, A.I. Medvedev, N.P. Kirda, $^{40}Ar/^{39}Ar$ dates from the West Siberian Basin Siberian flood basalt province doubled, Science 296 (2002) 1846–1849.

[10] D.H. Erwin, S.A. Bowring, J. Yugan, End-Permian mass extinction: A review, in: C. Koeberl, K.G. MacLeod (Eds.), Catastrophic Events and Mass Extinctions: Impacts and Beyond, Geol. Soc. Am. Spec. Paper 356 (2002) 363–383.

[11] V.L. Masaitis, Permian and Triassic volcanism of Siberia, Zapiski VMO, part CXII, issue 4 (1983) 412–425 (in Russian).

[12] V.A. Fedorenko, G.K. Czamanske, Results of new field and geochemical studies of the volcanic and intrusive rocks of the Maymecha-Kotuy area, Siberian flood-basalt province, Russia, Int. Geol. Rev. 39 (1997) 479–531.

[13] E.N. Lind, S.V. Kropotov, G.K. Czamanske, S.C. Gromme, V.A. Fedorenko, Paleomagnetism of the Siberian flood basalts of the Noril'sk area: A constraint on eruption duration, Int. Geol. Rev. 36 (1994) 1139–1150.

[14] V. Fedorenko, G. Czamanske, T. Zen'ko, J. Budahn, D. Siems, Field and geochemical studies of the melilite-bearing Arydzhangsky Suite, and an overall perspective on the Siberian alkaline-ultramafic flood-volcanic rocks, Int. Geol. Rev. 42 (2000) 769–804.

[15] J.D. Kramers, C.B. Smith, A feasibility study of U-Pb and Pb-Pb dating of kimberlites using groundmass mineral fractions and whole-rock samples, Isot. Geosci. 1 (1983) 23–38.

[16] C.B. Smith, H.L. Allsop, O.G. Garvie, J.D. Kramers, P.F.S. Jackson, C.R. Clement, Note on the U-Pb perovskite method for dating kimberlites: Examples from the Wesselton and De Beers mines, South Africa, and Somerset Island, Canada, Chem. Geol. 79 (1989) 137–145.

[17] L.M. Heaman, B.A. Kjarsgaard, Timing of North American kimberlite magmatism: continental extension of the Great Meteor hotspot track?, Earth Planet. Sci. Lett. 178 (2000) 253–268.

[18] M. Queen, L.M. Heaman, J.A. Hanes, D.A. Archibald, E. Farrar, $^{40}Ar/^{39}Ar$ phlogopite and U-Pb perovskite dating of lamprophyre dykes from the eastern Lake Superior region: Evidence for a 1.14 Ga magmatic precursor to Midcontinent Rift volcanism, Can. J. Earth Sci. 33 (1996) 958–965.

[19] C.B. Smith, T.C. Clark, E.S. Barton, J.W. Bristow, Emplacement ages of kimberlite occurrences in the Prieska region, southwest border of the Kaapvaal Craton, South Africa, Chem. Geol. 113 (1994) 149–169.

[20] P. Kinney, B.J. Griffin, L.M. Heaman, F.F. Brakhfogel, Z.V. Spetius, SHRIMP U-Pb ages of perovskite and zircon from Yakutian kimberlites, Russ. Geol. Geophys. 38 (1997) 97–105.

[21] N.T. Arndt, K. Lehnert, Yu.R. Vasil'ev, Meimechites: highly magnesian alkaline magmas from the subcontinental lithosphere?, Lithos 34 (1995) 41.

[22] K.M. Shikhorina, Volcanic formations of the Maymecha-Kotuy province, in: L.S. Egorov (Ed.), Carbonatites and Alkaline Rocks of Northern Siberia, NIIGA, Leningrad, 1970, pp. 5–14 (in Russian).

[23] T.E. Krogh, A low contamination method for hydrothermal decomposition of zircon and extraction of U and Pb for isotopic age determination, Geochim. Cosmochim. Acta 37 (1973) 485–494.

[24] R.L. Edwards, J.H. Chen, G.J. Wasserburg, ^{238}U-^{234}U-^{230}Th-^{232}Th systematics and the precise measurement of time over the past 500,000 years, Earth Planet. Sci. Lett. 81 (1986) 175–192.

[25] Y. Amelin, A.N. Zaitsev, Precise geochronology of phoscorites and carbonatites: the critical role of U-series disequilibrium in age interpretations, Geochim. Cosmochim. Acta 66 (2002) 2399–2419.

[26] K.R. Ludwig, Isoplot/Ex version 2.2, A geochronological toolkit for Microsoft Excel, Berkeley Geochron Center Spec. Publ. No.1a (2000).
[27] D.W. Davis, Optimum linear regression and error estimation applied to U-Pb data, Can. J. Earth Sci. 19 (1982) 2141–2149.
[28] L.J. Le Roux, L.E. Glendinin, Half-life of thorium-232, Nat. Conf. Nuclear Energy Appl. Isotop. Radiat. Proc., 1963, pp. 77–88.
[29] K. Ludwig, On the treatment of concordant uranium-lead ages, Geochim. Cosmochim. Acta 62 (1998) 665–676.
[30] R. Anczkiewicz, F. Oberli, J.P. Burg, I.M. Villa, D. Gunther, M. Meier, Timing of normal faulting along the Indus Suture in Pakistan Himalaya and a case of major $^{231}Pa/^{235}U$ initial disequilibrium in zircon, Earth Planet. Sci. Lett. 191 (2001) 101–114.
[31] J.M. Mattinson, Anomalous isotopic composition of lead in young zircons, Carnegie Inst. Washington Yearb. 72–73 (1973) 613–616.
[32] A.J. Naldrett, P.C. Lightfoot, V. Fedorenko, W. Doherty, N.S. Gorbachev, Geology and geochemistry of intrusions and flood basalts of the Noril'sk region, USSR, with implications for the origin of the Ni-Cu ores, Econ. Geol. 87 (1992) 975–1004.
[33] J.L. Wooden, G.K. Czamanske, V.A. Fedorenko, N.T. Arndt, C. Chauvel, R.M. Bouse, B.-S.W. King, R.J. Knight, D.F. Siems, Isotopic and trace-element constraints on mantle and crustal contributions to Siberian continental flood basalts, Norilsk area, Siberia, Geochim. Cosmochim. Acta 57 (1993) 3677–3704.
[34] J.J. Mahoney, M.J. Coffey, Large igneous provinces: continental, oceanic, and planetary flood volcanism, AGU Geophys. Monogr. 100 (1997) 438 pp.
[35] C.G. Farnetani, M.A. Richards, Numerical investigations of the mantle plume initiation model for flood basalt events, J. Geophys. Res. 99 (1994) 13813–13833.
[36] A.R. Basu, R.J. Poreda, P.R. Renne, F. Teichmann, Yu.R. Vasiliev, N.V. Sobolev, B.D. Turrin, High-^{3}He plume origin and temporal-spatial evolution of the Siberian flood basalts, Science 269 (1995) 822–825.
[37] G.K. Czamanske, A.B. Gurevitch, V. Fedorenko, O. Simonov, Demise of the Siberian plume: Paleogeographic and paleotectonic reconstruction from the prevolcanic and volcanic record, north-central Siberia, Int. Geol. Rev. 41 (1998) 95–115.
[38] V.I. Budnikov, Regularities of sedimentation in the Carboniferous and Permian of the Western Siberian Platform, Proceedings of SNIIGGiMS, Issue 183, Nedra Press, Moscow, 1976, 135 pp. (in Russian).
[39] D.L. Anderson, The edges of the mantle, in: M. Gurnis, M.E. Wysession, E. Knittle, B.A. Buffet (Eds.), The Core-Mantle Boundary Region, Geodynamics 28, Am. Geophys. Union, Washington, DC, 1998, pp. 255–271.
[40] V. Courtillot, C. Jaupart, I. Manighetti, P. Tapponnier, J. Besse, On causal links between flood basalts and continental breakup, Earth Planet. Sci. Lett. 166 (1999) 177–195.
[41] L.T.E. Tanton, B.H. Hager, Melt intrusion as a trigger for lithospheric foundering and the eruption of the Siberian flood basalts, Geophys. Res. Lett. 27 (2000) 3937–3940.
[42] B.F. Bohor, P.J. Modreski, E.E. Foord, Shocked quartz in the Cretaceous-Tertiary boundary clays: Evidence for a global distribution, Science 236 (1987) 705–709.
[43] G.A. Izett, The Cretaceous/Tertiary boundary interval, Raton Basin, Colorado and New Mexico, and its content of shock-metamorphosed minerals; Evidence relevant to the K-T boundary impact-extinction theory, Geol. Soc. Am. Spec. Paper 249 (1990) 100 pp.
[44] L.W. Alvarez, W. Alvarez, F. Asaro, H.V. Michel, Extraterrestrial cause for the Cretaceous/Tertiary extinction, Science 208 (1980) 1095–1108.
[45] A.R. Hildebrand, G.T. Penfield, D.A. Kring, M. Pilkington, Z.A. Camargo, S. Jacobsen, W. Boynton, Chicxulub crater: A possible Cretaceous-Tertiary boundary impact crater on the Yucatan Peninsula, Mexico, Geology 19 (1991) 867–871.
[46] T.E. Krogh, S.L. Kamo, V. Sharpton, L.E. Marin, A.R. Hildebrand, U-Pb ages of single shocked zircons linking distal K/T ejecta to the Chicxulub crater, Nature 366 (1993) 731–734.
[47] S.L. Kamo, T.E. Krogh, Chicxulub crater source for shocked zircon crystals from the Cretaceous-Tertiary boundary layer, Saskatchewan: Evidence from new U-Pb data, Geology 23 (1995) 281–284.
[48] L. Becker, R.J. Poreda, A.G. Hunt, T.E. Bunch, M. Rampino, Impact event at the Permian-Triassic boundary evidence from extraterrestrial noble gases in fullerenes, Science 291 (2001) 1530–1533.
[49] K.A. Farley, S. Mukhopadhyay, An extraterrestrial impact at the Permian-Triassic boundary? Comment, Science 293 (2001) 2343a.
[50] Y. Isozaki, An extraterrestrial impact at the Permian-Triassic boundary?, Science 293 (2001) 2343a.
[51] I. Metcalfe, R.S. Nicoll, R. Mundil, C. Foster, J. Glen, J. Lyons, X.F. Wang, C.Y. Wang, P.R. Renne, L. Black, Q. Xun, X.D. Mao, Episodes 24 (2001) 239–244.
[52] T. Braun, E. Osawa, C. Detre, I. Toth, On some analytical aspects of the determination of fullerenes in samples from the Permian-Triassic boundary layers, Chem. Phys. Lett. 348 (2001) 361–362.
[53] K. Kaiho, Y. Kajiwara, T. Nakano, Y. Miura, H. Kawahata, K. Tazaki, M. Ueshima, Z. Chen, G. Shi, End-Permian catastrophe by a bolide impact: Evidence of a gigantic release of sulfur from the mantle, Geology 29 (2001) 815–818.
[54] C. Koeberl, I. Gilmour, W. Reimold, P. Claeys, B. Ivanov, End-Permian catastrophe by bolide impact: Evidence of a gigantic release of sulfur from the mantle Comment, Geology 30 (2002) 855–856.
[55] D.H. Erwin, S.A. Bowring, J. Yugan, End-Permian mass extinctions: A review, in: C. Koeberl, K.G. MacLeod (Eds.), Catastrophic Events and Mass Extinctions: Impacts and Beyond, Geol. Soc. Am. Spec. Paper 356 (2002) 363–383.

[56] K. Min, R. Mundil, P.R. Renne, K.R. Ludwig, A test for systematic errors in $^{40}Ar/^{39}Ar$ geochronology through comparison with U/Pb analysis of a 1.1 Ga rhyolite, Geochim. Cosmochim. Acta 64 (2000) 73–98.
[57] R. Mundil, I. Metcalfe, K.R. Ludwig, P.R. Renne, F. Oberli, R.S. Nicoll, Timing of the Permian-Triassic biotic crisis: implications from new zircon U/Pb age data (and their limitations), Earth Planet. Sci. Lett. 187 (2001) 131–145.
[58] J.M. Mattinson, A study of complex discordance in zircons using step-wise dissolution techniques, Contrib. Mineral. Petrol. 116 (1994) 117–129.
[59] K. Faure, M.K. de Wit, J.P. Willis, Late Permian global coal hiatus linked to ^{13}C-depleted CO_2 flux into the atmosphere during the final consolidation of Pangea, Geology 23 (1995) 507–510.
[60] P.B. Wignall, R.J. Twitchett, Oceanic anoxia and the end Permian mass extinction, Science 272 (1996) 1155–1158.
[61] K. McCartney, A.R. Huffman, M. Tredoux, M., A paradigm for endogenous causation of mass extinctions, in: V.L. Sharpton, P.D. Ward (Eds.), Global Catastrophes in Earth History, Geol. Soc. Am. Spec. Paper 247 (1990) 125–138.
[62] T.M. Gerlach, E.J. Graeber, Volatile budget of Kilauea volcano, Nature 313 (1985) 273–277.
[63] K.G. Caldeira, M.R. Rampino, Deccan volcanism, greenhouse warming, and the Cretaceous-Tertiary boundary, in: V.L. Sharpton, P.D. Ward (Eds.), Global Catastrophes in Earth History, Geol. Soc. Am. Spec. Paper 247 (1990) 117–123.
[64] G.J. Retallack, A. Seyedolai, E.S. Krull, W.T. Holser, C.P. Ambers, F.T. Kyte, Search for evidence of impact at the Permian-Triassic boundary in Antarctica and Australia, Geology 26 (1998) 979–982.
[65] A. Baud, M. Margaritz, W.T. Holser, Permian-Triassic of the Tethys: Carbon isotope studies, Geol. Rundsch. 78 (1989) 649–677.
[66] D. Erwin, The Great Paleozoic Crisis: Life and Death in the Permian, Columbia Univ. Press, New York, 1993, 327 pp.
[67] S.P. Hasselbo, D.R. Gröcke, H.C. Jenkyns, C.J. Bjerrum, P. Farrimond, H.S. Morgans Bell, O.R. Green, Massive dissociation of gas hydrate during a Jurassic oceanic anoxic event, Nature 406 (2000) 392–395.
[68] E.S. Krull, G.J. Retallack, $\delta^{13}C$ depth profiles across the Permian-Triassic boundary: Evidence for methane release, GSA Bull. 112 (2000) 1459–1472.
[69] M.R. Rampino, A. Prokoph, A. Adler, Tempo of the end-Permian event: High resolution cyclostratigraphy at the Permian-Triassic boundary, Geology 28 (2000) 643–646.
[70] R.J. Twitchett, C.V. Looy, R. Morante, H. Visscher, P. Wignall, Rapid and synchronous collapse of marine and terrestrial ecosystems during the end-Permian biotic crisis, Geology 29 (2001) 351–354.
[71] A.H. Knoll, R.K. Bambach, D.E. Canfield, J.P. Grotzinger, Comparative earth history and late Permian mass extinction, Science 273 (1996) 452–457.
[72] P.B. Wignall, Large igneous provinces and mass extinctions, Earth Sci. Rev. 53 (2001) 1–33.
[73] G.K. Czamanske, http://geopubs.wr.usgs.gov/open-file/of02-074/ (2002).
[74] T.E. Krogh, Improved accuracy of U-Pb zircon ages by the creation of more concordant systems using an air abrasion technique, Geochim. Cosmochim. Acta 46 (1982) 637–649.